COMPARISON OF THE LOW-CYCLE FATIGUE PROPERTIES BETWEEN THE 6082-T6 AND 6061-T651 ALUMINIUM ALLOYS

Alfredo S. Ribeiro, aribeiro@utad.pt
Engineering Department, School of Science and Technology, University of Trás-os-Montes and Alto Douro
Quinta de Prados, 5001-801 Vila Real, Portugal
UCVE, IDMEC – Pólo FEUP, Rua Dr. Roberto Frias, 4200-465 Porto, Portugal

Luís P. Borrego, borrego@isec.pt
Department of Mechanical Engineering, ISEC
Rua Pedro Nunes, Quinta da Nora, 3030-199 Coimbra, Portugal

Abilío M. P. de Jesus, ajesus@utad.pt
Engineering Department, School of Science and Technology, University of Trás-os-Montes and Alto Douro
Quinta de Prados, 5001-801 Vila Real, Portugal
UCVE, IDMEC – Pólo FEUP, Rua Dr. Roberto Frias, 4200-465 Porto, Portugal

José Domingos M. Costa, josé.domingos@dem.uc.pt
Department of Mechanical Engineering, Faculty of Sciences and Technology, University of Coimbra
Pólo II, Pinhal de Marrocos, 3030-201 Coimbra, Portugal

Abstract. *In this study the low-cycle fatigue behaviours of the 6082-T6 and 6061-T651 aluminium alloys are characterized. These alloys are AlMgSi aluminium alloys and are intended for mechanical engineering applications, namely in steelwork, bridge building, shipbuilding, high pressure applications and others applications used in metallurgical industry. They show good welding characteristics. The low-cycle fatigue behaviours of the 6082-T6 and 6061-T651 aluminium alloys were evaluated using fully-reversible strain control fatigue tests (R=-1). The cyclic stress-strain curve, used to characterize the cyclic plastic response, was determined using one specimen for each strain level.*

Keywords: *AlMgSi aluminium alloys, low-cycle fatigue, stress-strain curves, cyclic behaviour.*

1. INTRODUCTION

This paper presents the main results of an investigation carried out with two AlMgSi materials, with different chemical compositions, namely the 6082 –T6 and 6061-T651 aluminium alloys. These designations are according to Aluminium Association Standards and Data Handbook (1976).

These alloys have moderate to high strength. However, if the weight/strength concept is taken into account, it can be concluded that the aluminium alloys presents advantages in some domains of engineering applications, such as a good corrosion resistance, good weldable characteristics, good formability. These properties are commonly used as advantages in the manufacture of heavy-duty structures in mechanical engineering, namely, in shipbuilding, bridge building, railroad cars, furniture, tank fittings, general structures, high pressure applications, hydraulic pistons, in pipelines and others applications used in metallurgical industry.

An experimental program based on fatigue tests of smooth specimens was undertaken for both aluminium alloys. The cyclic hardening/softening behaviour is assessed for both materials and the monotonic and cyclic curves are compared. Finally, the ductility and strength fatigue properties are evaluated from the test data.

2. STRAIN-LIFE RELATIONS

Low-cycle fatigue results are usually represented using relations between the strain amplitude and the number of reversals to failure, $2N_f$, usually considered to correspond to the initiation of a macroscopic crack (crack depth of 0.25 mm) (Costa, 1991). The most used relation to model low-cycle fatigue was proposed by Coffin (1954) and Manson (1953), which relates the plastic strain amplitude, $\Delta\varepsilon_p/2$, with the number of reversals to crack initiation, $2N_f$:

$$\frac{\Delta\varepsilon_p}{2} = \varepsilon_f^{'}\left(2N_f\right)^c \tag{1}$$

where ε_f' and c are, respectively, the fatigue ductility coefficient and fatigue ductility exponent. The Coffin-Manson relation can be extended to high-cycle fatigue domains using the relation proposed by Basquin (1953). This relation relates the elastic strain amplitude, $\Delta\varepsilon_e/2$, with the number of reversals to failure, $2N_f$:

$$\frac{\Delta\varepsilon_e}{2} = \frac{\Delta\sigma}{2E} = \frac{\sigma_f^{'}}{E}\left(2N_f\right)^{b} \tag{2}$$

where $\Delta\varepsilon_e/2$ is the elastic strain amplitude, $\sigma_f^{'}$ is the fatigue strength coefficient, b is the fatigue strength exponent and E is the Young's modulus. The number of reversals corresponding to the transition between low- and high-cycle fatigue regimes is characterised by total strain amplitude composed by equal components of elastic and plastic strain amplitudes. Lives below this transition value are dictated by ductility properties; lives above this transition value are dictated by strength properties. Morrow (1965) suggested the superposition of Eqs. (1) and (2), resulting in a more general equation, valid for low- and high-cycle fatigue regimes:

$$\frac{\Delta\varepsilon}{2} = \frac{\Delta\varepsilon_e}{2} + \frac{\Delta\varepsilon_p}{2} == \frac{\sigma_f^{'}}{E}\left(2N_f\right)^{b} + \varepsilon_f^{'}\left(2N_f\right) \tag{3}$$

Morrow and Tuller (1965) demonstrated that b e c exponents vary with the cyclic hardening exponent, n', having proposed the following relations:

$$c = \frac{1}{1+5n'}; \quad b = \frac{n'}{1+5n'} \tag{4}$$

Several authors have been suggesting relationships among ε_f' and ε_f, the fatigue ductility coefficient and the true strain obtained in a monotonic tensile test. The relationships are numerous, varying ε_f' among $0.35\varepsilon_f$ and ε_f, depending on material. Landgraf (1970) suggested for ε_f' the following relation:

$$\varepsilon_f^{'} = 0.002\left(\sigma_f / \sigma_{0.2}\right)^{1/n'} \tag{5}$$

where σ_f represents the tensile test and $\sigma_{0.2}$ the yield strength for 0.2% residual strain. The application of this relationship allows good results.

3. STRESS-STRAIN HYSTERESIS LOOPS ANALYSIS

Cyclic stress-strain curves are usually expressed using the Ramberg-Osgood (1943) relationship:

$$\frac{\Delta\varepsilon}{2} = \frac{\Delta\sigma}{2E} + \left(\frac{\Delta\sigma}{2k'}\right)^{\frac{1}{n'}} \tag{6}$$

where $\Delta\sigma$ is the stress range, $\Delta\varepsilon$ the strain range, E the Young Modulus, $k^{'}$ the cyclic hardening coefficient and n' the cyclic hardening exponent.

Although Eq. (6) represents the relationship between stress and strain stable amplitudes, it cannot, generally, describe the hysteresis loop branches. A material is said to exhibit Masing behaviour (Masing, 1926), if the magnification of the cyclic stress-strain curve equation by a factor of two describes the branches of the hysteresis loops (see schematic representation shown in Fig. 1). The origin of this curve is at the compressive tip of the correspondent loop. Furthermore, in Masing´s model, the stress-strain path after stress reversals follows a unique curve, regardless of the loading amplitude. It was observed that the 6061 and 6082 alloys show a non-Masing type behaviour.

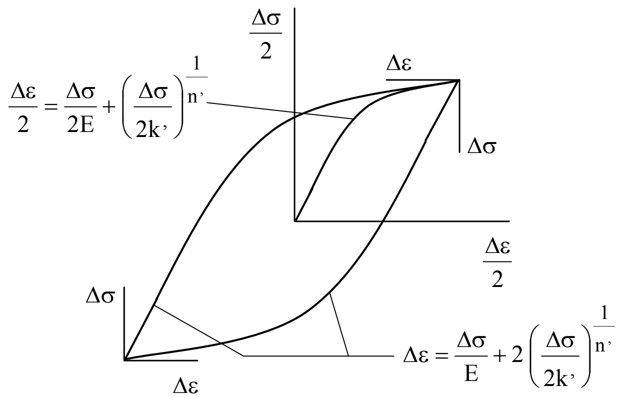

Figure 1**.** Masing type material.

4. EXPERIMENTAL PROGRAM

This research was conducted based on two distinct AlMgSi aluminium alloys: the 6082-T6 and 6061-T651 alloys. The 6061-T651 is a precipitation hardening aluminium alloy, containing magnesium and silicon as its major alloying elements. It has good mechanical properties and exhibits good weldability. It is one of the most common alloys of aluminium for general purpose use. The T651 treatment corresponds to stress-relieved stretch and artificially aging. The T6 treatment corresponds to a conversion of heat-treatable material to age-hardened condition by solution treatment, quenching and artificial age-hardening. The chemical composition of both materials, are shown in Tab. 1.

Table 1. Main chemical composition of the AlMgSi aluminium alloys (weight %).

Alloy	Si	Mg	Mn	Fe	Cr
6082 - T6	1.05	0.80	0.680	0.26	0.250
6061- T651	0.69	0.94	0.113	0.29	0.248

The 6082-T651 aluminium alloy investigated in this work was delivered in the form of extruded rounds with 20 mm diameter. The 6061-T651 investigated was delivered in the form of plates with 12 mm thickness. The microstructures are represented in Fig. 1.

The microstructure of the 6082-T6 presented in Fig. 2a) presents a good definition of the grain, with regular form, being possible the observation of phases including Si, Mg and Cr elements which are responsible by the good weldability, high hardness, corrosion resistance and high mechanical strenght.

The microstructure of 6061-T651 aluminium alloy (Fig. 2b)) is composed by a matrix rich in Al phase and a darker phase, with irregular form, in low amount, that corresponds to the Si. This alloy is perhaps one of the most versatile of heat treatable aluminium alloys. It was developed for applications involving moderate strength, good formability and weldability. Because of such desirable properties, this alloy is used in civilian and militaries industries.

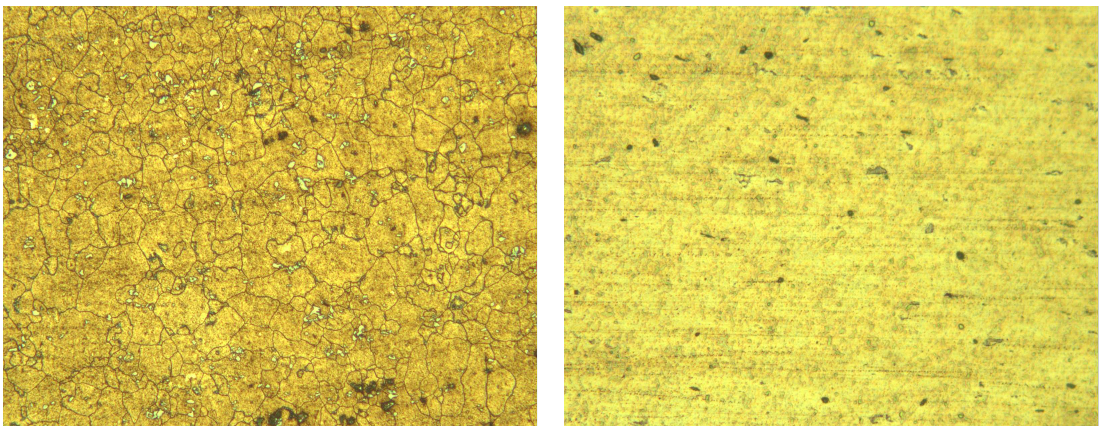

a) b)

Figure 2. Typical microstructure: a) Al 6082-T6 b) Al 6061-T651.

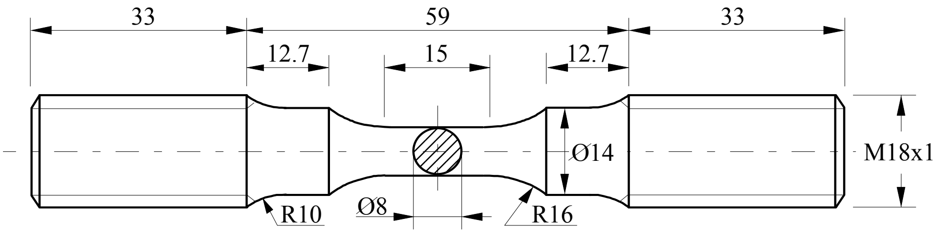

Figure 3. Geometry and dimensions of the specimens used in the low-cycle fatigue tests (dimensions in mm).

The experimental program included low-cycle fatigue tests of small round specimens of 8 mm diameter. The geometry and dimensions of the specimen used in the low-cycle fatigue tests is represented in Fig. 2 and are in agreement with the recommendations of ASTM E606 (ASTM, 1998). After machining, the specimen surfaces were mechanically polished. All the major geometry and dimensions of the specimens are illustrated in Fig. 2. The experiments were carried out in a close-loop mechanical test machine, with 100 kN capacity, interfaced to a computer for machine control and data acquisition. A sinusoidal waveform was used as command signal. The fatigue tests, in all series, were conducted with constant strain amplitudes, at room temperature in air. The longitudinal strain was measured using a longitudinal extensometer with a base length equal to 12.5 mm and limit displacements of ±2.5 mm.

The specimen were cyclic loaded under strain control with symmetrical push-pull loading, with a nominal strain ratio R_ε= -1. The nominal strain rate $d\varepsilon/dt$ was kept constant in all specimens at the value $8\times10^{-3}\ s^{-1}$ in order to avoid any influence of the strain rate on the hysteresis loop shape. The testing frequency was then calculated as a function of the strain amplitude, $\Delta\varepsilon/2$, by the following equation:

$$f = \frac{d\varepsilon / dt}{4\left(\Delta\varepsilon / 2\right)} \tag{7}$$

The cyclic stress-strain curves were determined using the method of one specimen for each imposed strain level and defining the stable hysteresis cycle as the cycle at which the specimens reached 50% of the fatigue life. The specimens were tested with imposed strain ranges between 0.32% and 4% for the 6082-T6 and 0.9% to 3.5% strain ranges for the 6061-T651. The monotonic stress-strain curves were also experimentally determined for comparison.

5. RESULTS AND DISCUSSION

The monotonic strength and elastic properties of the 6082-T6 and the 6061-T651 aluminium alloys are represented in Tab. 2, (Borrego *et al* (2008) and Ribeiro *et al* (2008). It is possible to realize similar properties for both materials under research. However, a detailed comparison reveals that the 6082-T6 alloy presents better monotonic strength than the 6061-T651 alloy, with slightly lower ductility.

Table 2. Monotonic strength and elastic properties of the 6082-T6 and 6061-T651 aluminium alloys.

Properties	6082-T6	6061-T651
Tensile strength, σ_{UTS} (MPa)	330	317
Yield strength, $\sigma_{0.2\%}$ (MPa)	307	279
Elongation, ε_r (%)	9	10.0
Young modulus, *E* (GPa)	70	68.0
Poisson coefficient, ν	0.33	0.33

For fully-reversed strain-controlled fatigue tests, the stress amplitude is plotted against the number of cycles in Fig. 4 for both materials (Borrego *et al* (2008) and Ribeiro *et al* (2008). For low strain amplitudes ($\Delta\varepsilon/2<0.8\%$) the 6082 alloy, Fig 4a, showed cyclic softening, whereas for high strain amplitudes ($\Delta\varepsilon/2>0.9\%$) cyclic hardening was observed. For intermediate strain amplitudes ($0.8\%\leq \Delta\varepsilon/2\leq 0.9\%$) the initial hardening stage is followed by long term cyclic softening. In any case, the initial phase of cyclic hardening represented only between 4% and 7% of the fatigue life. The hardening rate, increase rate of the stress amplitude, with strain cycles increased with strain range. Furthermore, the softening rate, decrease rate of the stress amplitude with strain cycles, increases as the strain range decreases.

The 6061-T651 aluminium alloy did not present a significant cyclic hardening, verifying only the occurrence of cyclic softening for strains ranges bellow of 1.0%. For values of $\Delta\varepsilon/2>1\%$ cyclic hardening occurs, being its increasing importance with the increase of $\Delta\varepsilon/2$. Figure 5 illustrates the hardening behaviour comparing the cyclic curve with the monotonic curve of the materials.

Figure 6 presents the total strain amplitude versus life curves obtained from the superposition of the elastic and plastic strain amplitude versus life curves. The number of reversals of transition, $2N_f$, verified for 6082-T6 and for the 6061-T651 aluminium alloys were 744 and 969 reversals. The fatigue ductility and strength properties of the alloys were obtained from Fig. 6. Therefore, the strain-fatigue life of the analysed alloys, taking into account the mean stress, σ_m, effect by application of Morrow's equation is given, for 6082-T6 and 6061-T651 alloys, respectively by:

$$\frac{\Delta\varepsilon}{2} = \frac{487 - \sigma_m}{70\,000}\left(2N\right)^{-0.07} + 0.209\left(2N\right)^{-0.593} \tag{8}$$

$$\frac{\Delta\varepsilon}{2} = \frac{394 - \sigma_m}{68000}\left(2N\right)^{-0.045} + 0.157\left(2N\right)^{-0.723} \tag{9}$$

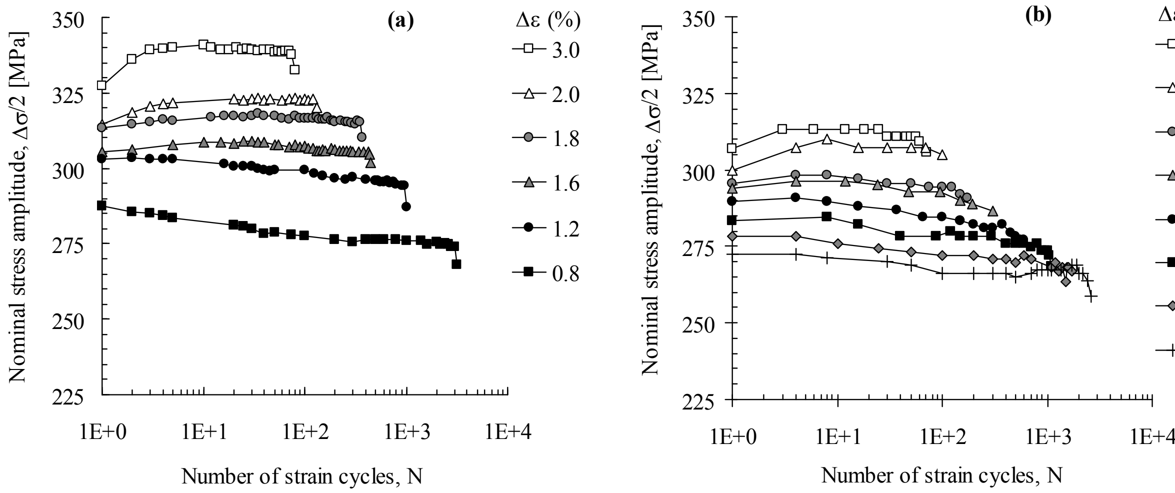

Figure 4. Stress amplitude *versus* number of cycles for fully-reversed strain-controlled tests: (a) alloy 6082-T6, (b) alloy 6061-T651.

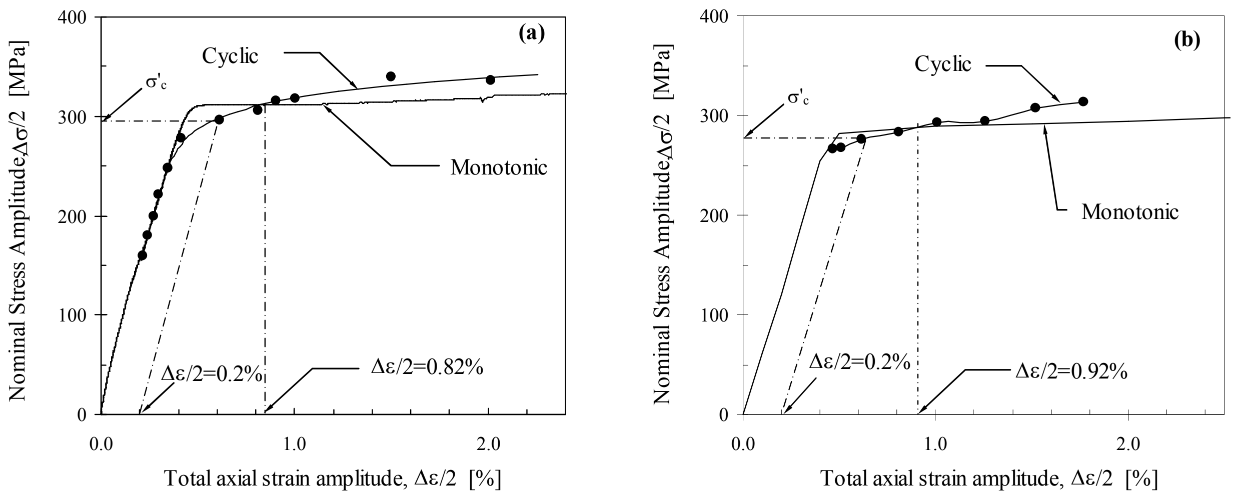

Figure 5. Monotonic and cyclic stress-strain curves: (a) alloy 6082-T6, (b) alloy 6061-T651.

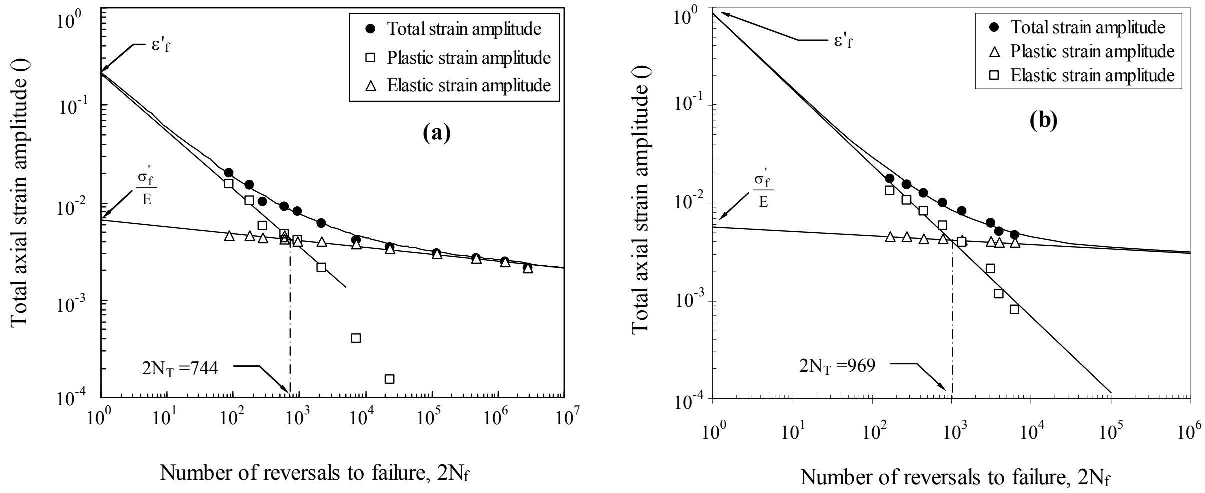

Figure 6. The total strain amplitude versus life curve obtained from the superposition of the elastic and plastic strain amplitude versus life curves: (a) alloy 6082-T6, (b) alloy 6061-T651.

Table 3 gives the coefficients of the Coffin-Manson and Basquin relations, as well as the parameters to the cyclic elastoplastic curves, according to the Ramberg-Osgood (1943), for the 6082-T6 and the 6061-T651 aluminium alloys.

Table 3. Coefficients of Coffin-Manson and Basquin relations and parameters of the cyclic curves obtained for the 6082-T6 and for the 6061-T651 aluminium alloys.

Properties	**6082-T6**	**6061-T651**
Fatigue strength coefficient, σ'_f [MPa]	487	394
Fatigue strength exponent, b	-0.07	-0.045
$b = n'/(1+5n')$	-0.048	-0.047
Fatigue ductility coefficient, ε'_f (-)	0.209	0.634
$\varepsilon_f = \varepsilon'_f/0.35$	0.597	1.335
$\varepsilon'_f = 0.35\varepsilon_f$	-	0.467
Fatigue ductility exponent, c	-0.593	-0.723
$c = 1/(1+5n')$ [-]	0.595	-0.763
σ'_f / E	0.0067	0.0058
Cyclic strain hardening coef., K' [MPa]	444	404
Cyclic strain hardening exp., n'	-0.064	-0.062
$n' = b/c$	-0.118	-0.062

6. CONCLUSIONS

The comparison between the low-cycle fatigue properties of two AlMgSi alloys, with different chemical composition, was carried out in this paper, and the following conclusions can be drawn:

- The monotonic strength and elastic properties of the 6082-T6 and 6061-T651 aluminium alloys are very similar.

- Cyclic softening and hardening for axial strain amplitudes respectively lower and higher than 0.82% were observed for alloy 6082-T6. The 6061-T651 aluminium alloy did not present a significant capacity of cyclic hardening, verifying exactly the occurrence of cyclic softening for strains ranges bellow of 1.0%. For values of $\Delta\varepsilon/2>1\%$ cyclic hardening occurs, being its increasing importance with the increase of $\Delta\varepsilon/2$.

- The ductility and strength fatigue properties of both alloys were experimentally determined. The transition fatigue life was found to be about 744 and 969 cycles for alloys 6082 T6 and 6061-T651, respectively.

- Non-Masing behaviour was observed for both materials. However, for alloy 6082 T6, the Masing model can still be used for strain ranges up to 1.5%.

7. REFERENCES

Aluminium Standards and Data Aluminium Association, New York, 1976.

American Society for Testing and Materials, 1998, “ASTM E606-92: Standard Practice for Strain-Controlled Fatigue Testing”, In Annual Book of ASTM Standards, Part 10, pp. 557-571.

Basquin, O. H., 1910, “The Exponential Law of Endurance Tests”, Proceedings of ASTM, 10 (II), pp. 625-630.

Borrego, L. P., Abreu, L. M., Costa, J. M. and Ferreira, J. M., 2004, “Analysis of Low Cycle Fatigue in AlMgSi Aluminium Alloys”, Engineering Failure Analysis, Vol. 11, pp. 715-725.

Coffin, L.F., 1954, “A study of the Effects of Cyclic Thermal Stresses on a Ductile Metal”, Translations of the ASME, Vol. 76(6), pp. 931-950.

Costa, J. D., 1991, “Análise da Tolerância de Defeitos em Ligas de Alumínio", PhD Thesis, FCTUC, Coimbra.

Landgraf, R.W., 1970, “The Resistance of Metals to Cycle Deformation”, ASTM STP 467, pp. 3-36.

Manson, S.S., 1953, “Behaviour of Materials Under Conditions of Thermal Stress”, Technical Report Nº.1170, National Advisory Committee for Aeronautics.

Morrow J. D., 1965, “Cyclic Plastic Strain Energy and Fatigue of Metals”, In Internal Friction, Damping and Cyclic Plasticity, ASTM STP 378, American Society for Testing and Materials, Philadelphia, PA, pp. 45-87.

Morrow, J.D., Tuler, F.R., 1965, “Low Cycle Fatigue Evaluation of Inconel 713C and Waspaloy”, Journal of Basic Engineering, Vol. 87, Nº 2, pp. 275-289.

Ramberg, W., and Osgood, W. R., 1943, “Description of Stress-Strain Curves by Three Parameters”, Technical Report No. 902, National Advisory Committee for Aeronautics, NACA.

Ribeiro, A.S., De Jesus A.M.P., Pereira H.F.S.G., Fernandes A.A., 2008, “Comparison of the Fatigue Properties of the P355NL1 Steel and the Al 6061-T651 Aluminium Alloy”, 11th Portuguese Conference on Fracture, R.F.Martins et al Editions, ISBN 978-989-95683-0-3-851, Faculty of Science and Technology of The New University of Lisbon, pp. 255-263, Portugal.

8. RESPONSIBILITY NOTICE

The authors are the only responsible for the printed material included in this paper.